Organic acid concentration thresholds for ageing of carbonate minerals: implications for CO_2 trapping/storage

Muhammad Ali[a,g*], Sarmad Al-Anssari[b,f], Muhammad Arif[a,e], Ahmed Barifcani[a,b], Mohammad Sarmadivaleh[a], Linda Stalker[c], Maxim Lebedev[d], Stefan Iglauer[a,g]

[a] Department of Petroleum Engineering, Curtin University, 26 Dick Perry Avenue, 6151 Kensington, Western Australia

[b] Department of Chemical Engineering, Curtin University, Kent Street, 6102 Bentley, Western Australia

[c] Commonwealth Scientific and Industrial Research Organisation (CSIRO), 26 Dick Perry Avenue, 6151 Kensington, Wester Australia

[d] Department of Exploration Geophysics, Curtin University, 26 Dick Perry Avenue, 6151 Kensington, Western Australia

[e] Department of Petroleum Engineering, University of Engineering and Technology, G. T. Road, Lahore 54890, Pakistan.

[f] Department of Chemical Engineering, University of Baghdad, Baghdad, 10071, Iraq.

[g] School of Engineering, Edith Cowan University, 270 Joondalup Drive, Joondalup, WA 6027 Australia

[*]corresponding author (Muhammad.ali7@postgrad.curtin.edu.au)

Highlights:

- Carbonate aquifers (Calcite Surfaces)
- Dissolution of organic acid components in crude oil (Stearic Acid)
- CO_2 trapping in deep saline aquifers and depleted hydrocarbon reservoirs and their associated risk in the presence of organic acid components

Keywords:

Wettability, CO_2 storage, Organic acids

Abstract

Hypothesis: CO_2 geological storage (CGS) involves different mechanisms which can store millions of tonnes of CO_2 per year into depleted hydrocarbon reservoirs and deep saline aquifers. But their storage capacity is influenced by the presence of different carboxylic compounds in the reservoir. These molecules strongly affect the water wetness of the rock, which has a dramatic impact on storage capacities and containment security. However, precise understanding of how these carboxylic acids influence the rock's CO_2-wettability is lacking.

Experiments: We thus systematically analysed these relationships as a function of pressure, temperature, storage depth and organic acid concentrations. A particular focus was on identifying organic acid concentration thresholds above which storage efficiency may get influenced significantly.

Findings: These thresholds (defined for structural trapping as a water contact angle $\theta > 90°$; and for capillary trapping when primary drainage is unaffected, i.e. $\theta > 50°$) were very low for structural trapping ($\sim 10^{-3} - 10^{-7}$ M organic acid concentration $C_{organic}$) and extremely low for capillary trapping (10^{-7} M to below 10^{-10} M $C_{organic}$). Since minute organic acid concentrations are always present in deep saline aquifers and certainly in depleted hydrocarbon reservoirs, significantly lower storage capacities and containment security than previously thought can be predicted in carbonate reservoirs, and reservoir-scale models and evaluation schemes need to account for these effects to de-risk CGS projects.

1. Introduction

Depleted hydrocarbon reservoirs and deep saline aquifers are potential CO_2 sinks in which anthropogenic CO_2 emissions can be stored, thus mitigating global warming.[1,2] Efficient and safe CO_2 geological storage involves a qualitative and quantitative assessment of the

contribution of the different functional trapping mechanisms which prevent the buoyant CO_2 from migrating back to the surface.[1]

In this context it has been shown that CO_2-wet surfaces drastically reduce structural[3-5] and capillary trapping capacities.[6-9] Furthermore, it is clear that organic acid content on the rock surface is the main factor which renders (originally strongly water-wet) mineral surfaces to become CO_2-wet.[4] While clean mineral surfaces are weakly, strongly or completely water-wet,[10-13] organic acid surfaces, e.g. alkylated or arylated minerals, minerals aged in crude oil or coal[4,5,14,15] are weakly, strongly or even completely CO_2-wet depending on pressure, temperature and brine salinity.[4,16,17]

However, chemically clean mineral surfaces are artificial in the sense that they can only be prepared and persist in strongly oxidising environments (e.g. in oxygen plasma or in UV-ozone atmosphere),[18,19] while it is well established that in the subsurface anoxic or reducing conditions prevail.[20,21]

In addition, it is clear that storage formations always contains traces of dissolved organic acid material,[22-27] which is potentially sufficient to significantly change the rock's CO_2-wettability. Indeed a partial mono-molecular layer adsorbed to the mineral surface would be sufficient for this.[19,28-33] Such organic acid contaminations thus has the potential to drastically reduce storage capacities and containment security.[5,9,34,35] It is therefore of vital importance to gauge this effect and to identify threshold concentrations of organic acid molecules at which CO_2 storage is significantly affected.

We thus systematically investigated such threshold values per clearly defined laboratory experiments; and we analysed the impact such minute organic acid concentrations have on CO_2 storage capacities and containment security.

2. Experimental Methodology

2.1. Materials

Nine pure calcite samples (Iceland spar, from WARD'S Natural Science, sample dimensions = 1 cm x 1 cm x 0.3 cm) were used as a model limestone storage formation. The surface roughnesses of all nine surfaces were measured via Atomic Forces Microscopy (AFM instrument model DSE 95-200, Semilab).

CO_2 (purity = 99.999 mol%; from BOC, gas code-082), N_2 (purity = 99.999 mol%; from BOC, gas code-234) and 10 wt% NaCl brine (NaCl purity ≥ 99.9 mol%; from Scharlab) were used. The NaCl was dissolved in deionized water (Ultrapure from David Gray; electrical conductivity = 0.02 mS/cm), which was equilibrated with calcite by rigorously mixing with calcite off-cuts while continuously monitoring the pH value.[36,37] Subsequently the NaCl brine was equilibrated with CO_2 at experimental conditions in a high pressure mixing reactor.[38]

Acetone (99.9 mol%; from Rowe Scientific) was used as surface cleaning agent, drops of hydrochloric acid (ACS reagent, concentration 37 vol%, Sigma Aldrich) were used to control the pH of the brine (see ageing procedure below for more details) and stearic acid (≥ 98.5 mol%; from Sigma Aldrich) was selected as a model for organic acid molecules present in the subsurface.[25,39-42]

2.2. Simulating real aquifer conditions

As mentioned above, real aquifers contain organic acid molecules which are partially adsorbed on the rock surface.[22-27] It is thus vital to re-create such mineral surfaces to realistically mimic aquifer rock surfaces, particularly with respect to their wettability characteristics.[28,43-45] Thus below the procedure for preparing such realistic aquifer surfaces is described, as it was used in this research work.

2.2.1 Calcite surface preparation

Initially the mineral (calcite) substrates were cleaned with calcite-equilibrated DI-water to remove any dust or surface fragments from the surface. The sample was then dried in an oven at 90°C for 60 mins and exposed to air plasma (using a Diemer Yocto instrument) for 15 mins to remove any organic contamination.[18,19]

Ageing procedure

To mimic a typical storage formation, where the rock pore surfaces were exposed to formation water over geological times[40-50] we adopted the following strategy:

The calcite samples were immersed for 30 mins in calcite-equilibrated 2 wt% NaCl brine (NaCl purity ≥ 99.9 mol%; from Scharlab) at ambient conditions, while the acidity was maintained at pH = 4 by adding drops of aqueous hydrochloric acid; this procedure increases the adsorption rate of stearic acid onto the substrate, and thus simulates adsorption of organic acid molecules over geological times (i.e. millions of years exposure time).[40-50] Ultraclean N_2 was then used to mechanically clean (blow away) the remaining water from the surface to avoid contamination. Subsequently the substrates were aged in stearic acid/n-decane solutions of prescribed molarity (10^{-2} M to 10^{-10} M stearic acid concentration) for seven days to mimic exposure to formation fluid (which contains organic acid molecules) over geological times.[39,40,51,52] Note that it is also shown that carboxylic acids and hydrocarbons both exist in deep saline aquifers[53], as a result of biodegradation and organic matter diagenesis and subsequent migration into the water zones.[54]

Mechanistically, the stearic acid esterifies the hydroxyl groups on the calcite surface in a condensation reaction (Scheme 1).[55-59]

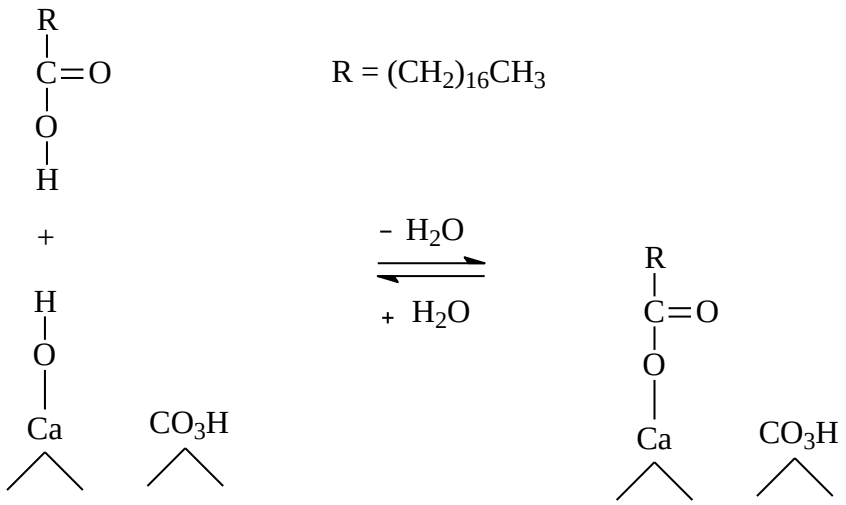

Scheme 1. Chemisorption of stearic acid ($CH_3(CH_2)_{16}$-COOH) on solid calcite surface (∧ indicates solid bulk).[55-59]

Thus octadecanoate groups (C_{18} ester groups) were chemically (covalently) bonded to the calcite surface, rendering them strongly hydrophobic.[60]

2.2.2. Surface characterization of pure and aged calcite surfaces

Pure calcite

The surface properties of the calcite samples were investigated via energy dispersive X-ray spectroscopy (EDS, Oxford X-act SSD X-ray detector with Inca and Aztec software), atomic force microscopy (AFM DSE 95-200, Semilab) and contact angle (θ) measurements. For pure calcite surfaces, the average atomic surface content was 24.7 wt% ± 4.9 wt% Ca, 20.5 wt% ± 3.3 wt% C and 54.8 wt% ± 6.3 wt% O, Table 1, Figure 2; these values are averages over 45 data points measured on five different surface sites for each of the nine samples. The average root mean square (RMS) surface roughness measured was 20.12 nm (± 16 nm), Table 2; which is very smooth. For such smooth surfaces no significant influence on CO_2-wettability was observed.[17] Furthermore, contact angles on these pure calcite samples were (advancing 0° and

receding 0°) at ambient conditions, thus pure calcite was completely water-wet at ambient conditions. However, higher contact angles (advancing 48° and receding 40°) and (advancing 68° and receding 62°) were measured at reservoirs conditions on these pure calcite samples (323 K, 10 MPa and 25 MPa), consistent with literature data.[61,62]

Aged calcite

Aging had no significant influence on surface roughness (20.58 nm ± 16 nm), Table 2. However, the atomic surface concentrations changed due to chemisorption of the carboxylic acids on the calcite surface, consistent with Zullig and Morse (1988).[42] The new average surface atomic content of the treated samples was 22.7 wt% ± 5.1 wt% Ca, 22.9 wt% ± 3.6 wt% C and 54.4 wt% ± 5 wt% O, Table 1, Figure 2. Thus, a significant overall average increase in surface carbon concentration (+2.3 wt% C) was observed due to surface stearate adsorption (Table 1).

Furthermore, aging of the calcite surfaces caused a significant change in contact angles and thus CO_2-wettability, this is discussed in detail below.

Table 1. Surface composition of pure and aged calcite and change due to ageing.

Stearic Acid Concentration (Molarity)	Pure calcite			After ageing			Change due to ageing			Estimated surface coverage[14]
	wt% Ca	wt% C	wt% O	wt% Ca	wt% C	wt% O	wt% Ca	wt% C	wt% O	$\left(1-\frac{wt\%\ C_{before\ aging}}{wt\%\ C_{after\ aging}}\right)\times 100$
10^{-2}	24.9	18.8	56.3	23.2	22.3	54.5	-1.7	+3.5	-1.8	15.7
10^{-3}	25.8	18.4	55.9	23.2	21.5	55.3	-2.6	+3.1	-0.6	14.4
10^{-4}	25.1	21.3	53.6	24.8	24.5	50.7	-0.3	+3.2	-2.9	13.1
10^{-5}	22.0	20.0	58.0	21.6	22.9	55.5	-0.4	+2.9	-2.5	12.7
10^{-6}	28.0	24.9	47.2	22.1	27.9	50.0	-5.9	+3.0	+2.8	10.8
10^{-7}	24.0	20.4	55.7	22.5	22.0	55.5	-1.5	+1.6	-0.2	7.3
10^{-8}	25.6	20.0	54.4	20.9	21.4	57.8	-4.7	+1.4	+3.4	6.5
10^{-9}	28.3	19.6	52.1	28.2	20.8	51.0	-0.1	+1.2	-1.1	5.8
10^{-10}	18.6	21.5	59.8	18.0	22.6	59.4	-0.6	+1.1	-0.4	4.9
0	20.9	20.1	59.0	20.9	20.1	59.0	0	0	0	0

Table 2. Contact angle measurements and Surface Roughness (AFM*) at different stearic acid concentrations

Stearic acid concentration (Molarity)	Initial RMS* surface roughness (nm), pure calcite	Final RMS* surface roughness (nm), treated calcite	CO_2/Calcite/brine contact angle (10 MPa and 323 K)		CO_2/Calcite/brine contact angle (25 MPa and 323 K)	
			θ_a	θ_r	θ_a	θ_r
10^{-2}	4.4	4.8	126.0 $^{n=3}$	98.6 $^{n=3}$	141.2 $^{n=3}$	131.8 $^{n=3}$
10^{-3}	13.4	13.9	108.2 $^{n=3}$	91.8 $^{n=3}$	113.5 $^{n=3}$	105.1 $^{n=3}$
10^{-4}	25.3	26.2	100.9 $^{n=3}$	86.5 $^{n=3}$	108.5 $^{n=3}$	101.8 $^{n=3}$
10^{-5}	37.1	37.6	72.4 $^{n=3}$	65.7 $^{n=3}$	99.6 $^{n=3}$	84.4 $^{n=3}$
10^{-6}	25.9	26.4	63.9 $^{n=3}$	53.5 $^{n=3}$	95.4 $^{n=3}$	81.7 $^{n=3}$
10^{-7}	27.2	27.5	60.9 $^{n=3}$	51.4 $^{n=3}$	87.5 $^{n=3}$	79.6 $^{n=3}$
10^{-8}	18.6	19.2	56.4 $^{n=3}$	49.7 $^{n=3}$	78.2 $^{n=3}$	68.8 $^{n=3}$
10^{-9}	7.2	7.5	52.0 $^{n=3}$	45.6 $^{n=3}$	71.8 $^{n=3}$	67.5 $^{n=3}$
10^{-10}	21.6	22.1	50.2 $^{n=3}$	43.1 $^{n=3}$	70.1 $^{n=3}$	64.3 $^{n=3}$

*RMS – Route Mean Square

*AFM - Atomic Force Microscopy

n - The number of repeated experiments at the conditions indicated

2.2.3 Contact angle measurements

CO_2-wettability was determined by contact angle measurements at reservoir conditions (i.e. 323 K, at 10 MPa and 25 MPa) using a tilted plate goniometric setup.[60,63] The experimental setup consisted of a high pressure-high temperature cell that can operate at reservoir conditions. The substrate was placed in a tilted angle of (17º) inside the cell. Two separate high precision syringe pumps (Teledyne D-500, pressure accuracy of 0.1%) adjusted the CO_2 pressure, or injected the brine. The detailed setup has been described earlier.[61,64]

Experimentally, the sample was placed inside the pressure cell on the tilted plate and the cell was heated to the desired temperature (323 K). Subsequently the CO_2 pressure was raised to prescribed values (10 MPa and 25 MPa), and a droplet of degassed brine with an average volume of 6 µL (± 1 µL) was dispensed onto the calcite surface through a needle. The advancing (θ_a) and receding (θ_r) water contact angles were then measured at the leading and trailing edge of the droplet just before the drop started to move.[63] A high-resolution video camera (Basler scA 640–70 fm, pixel size = 7.4 µm; frame rate = 71 fps; Fujinon CCTV lens:

HF35HA-1B; 1:1.6/35 mm) captured movies of these processes, and θ_a and θ_r were measured on images extracted from the movie files. The standard deviation of the measurements was ±3° based on replicated measurements.

3. Results and Discussion

CO_2-wettability of a storage formation is a key parameter which strongly influences CO_2 movement and distribution throughout the formation,[9,34] rate of injectivity,[4,5] storage capacity and containment security.[35,64,65] It is thus vital to understand CO_2-wettability in detail. In this context, the water receding contact angle (i.e. CO_2 displacing water) is related to structural trapping (below an impermeable caprock).[13] The advancing contact angle (water displacing CO_2) determines the capillary trapping capacity[66] and thus the amount of residually trapped CO_2.[6-8] It has also been shown in previous studies that dissolution trapping is significantly affected by the wettability, and it is thus necessary to know the wettability for accurate reservoir simulations and storage capacity predictions.[9,34]

We thus conducted contact angle measurements with different mineral surface chemistry scenarios at various thermo-physical conditions. The minute concentrations of stearic acid exposed to the substrates (which represents the small amounts of organic acid molecules in deep saline aquifer storage formations) had a highly significant influence on the water-wetness of the rock.

The results show that calcite rapidly loses its water-wetness with increasing stearic acid surface coverage (Figure 1), i.e. higher organic acid concentration led to significantly higher CO_2-wettability. For instance, at 323 K and 25 MPa, a carbonate storage formation having 10^{-10} M stearic acid is weakly water-wet (θ_r = 64.3°), while θ_r reached 90° at 10^{-4} M stearic acid exposure concentration (note that capillary leakage is possible at $\theta_r > 90°$).[4,5,65,67]

The optimal capillary trapping limit, which we define here as the point where primary drainage is unaffected by wettability is at θ_a = 50°.[68] θ_a is even more affected by the carboxylic acids concentration; even at a relatively low pressure of 10 MPa (note that increasing pressure increases θ)[4,17] and 323 K, θ_a reaches 50° at 10^{-10} M carboxylic acids concentration (note that this is a very minute concentration, much higher carboxylic acids concentration are measured in deep saline aquifers[22-27] and for 25 MPa this organic threshold is even below 10^{-10} M (Figure 1).

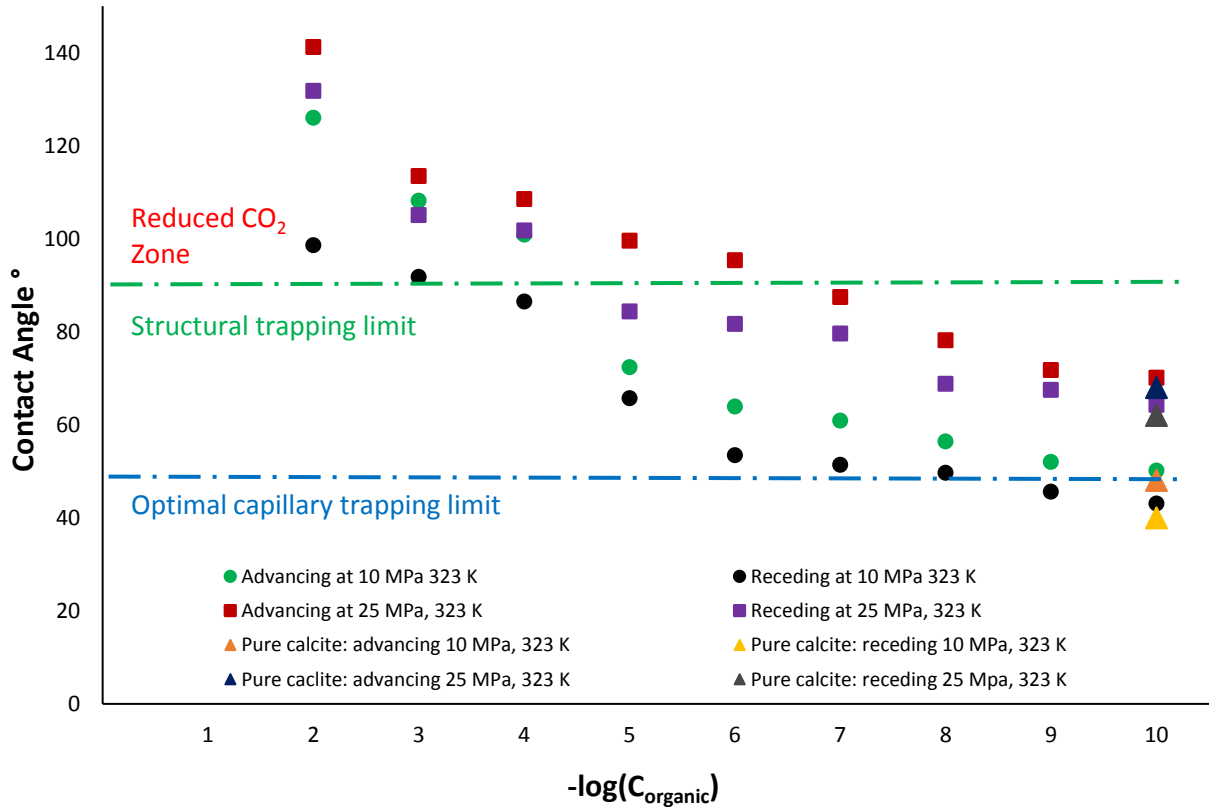

Figure 1: CO_2/calcite/brine (water) contact angles measured as a function of stearic acid concentration at 323 K and 10 MPa and 25 MPa; $C_{organic}$ is the stearic acid concentration (molarity). Dotted green line represents the structural trapping limit, while the blue dotted line represents the optimal capillary trapping limit. The zone above the dotted green line indicates the reduced CO_2 zone.

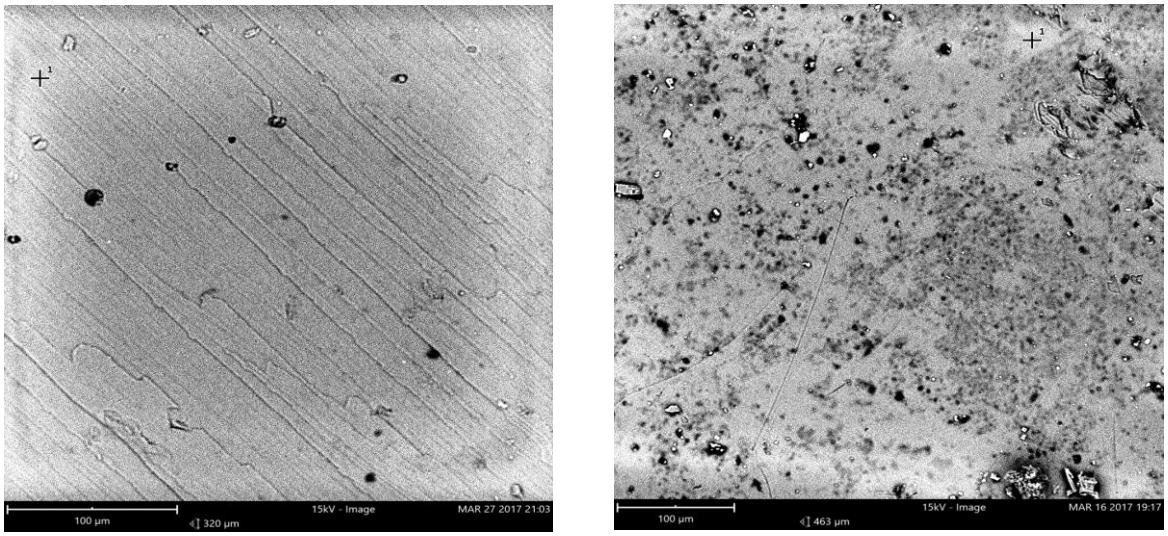

a) b)

Figure 2: SEM images before and after treatment with 10^{-2} M organic acid, (a) before treatment, (b) after treatment

The SEM images of the calcite surfaces were acquired before and after treatment with stearic acid; two examples are shown in Figure 2. It is clear that the texture of the image without stearic acid (Figure 2a) is quite transparent whereas a clear spread of organic acid on the calcite surface can be observed after surface treatment with 10^{-2} M stearic acid (Figure 2b). This stearic acid coverage of the calcite surface is responsible for the wettability change from strongly water-wet to weakly CO_2-wet

Physically, the shape of the droplet spreading on the calcite surface observed during the contact angle measurement also indicates the wetting behaviour (Figure 3). It is clear that the brine droplet almost completely spread on the pure calcite surface at 10 MPa (Figure 3a), implying water-wet conditions. On the contrary, the brine droplet only showed a minimal spread on the surface treated with 10^{-2} M stearic acid (measured at 25 MPa; Figure 3d) resulting in a higher water contact angle.

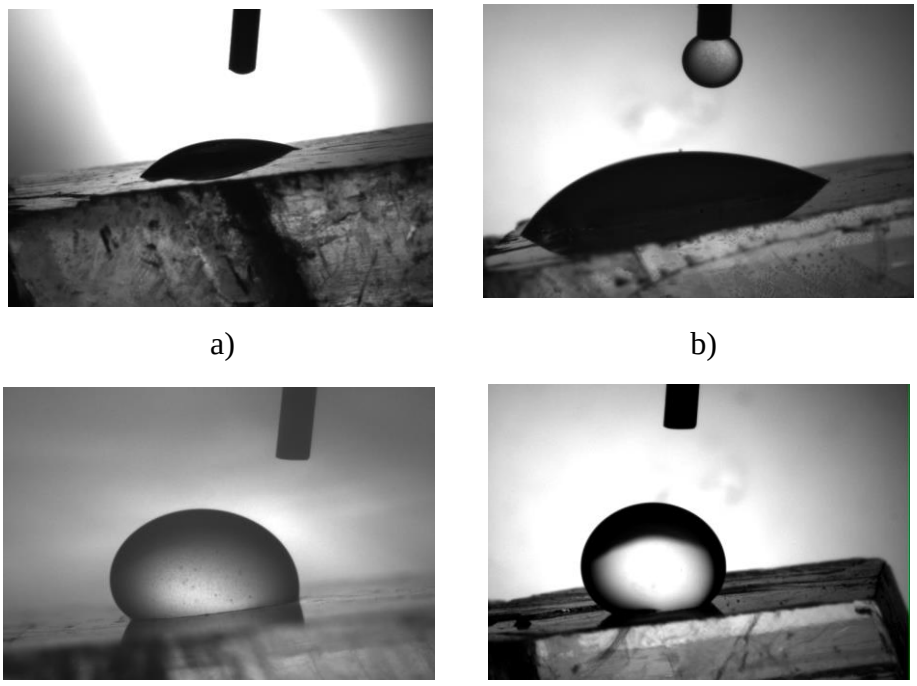

Figure 3: Contact angle images of different calcite surfaces, (a) pure calcite at 10 MPa, (b) pure calcite at 25 MPa, (c) aged calcite with 10^{-2} M organic acid at 10 MPa, (d) aged calcite with 10^{-2} M organic acid at 25 MPa

The implications of the results can be investigated via a capillary force – buoyancy force balance[69] as follows:

$$h = \frac{2\gamma cos\theta_r}{\Delta\rho g R} \qquad Eq.1$$

where 'h' is the height of the CO_2 column immobilized beneath the seal layer, 'γ' is CO_2-brine interfacial tension, 'θ_r' is the receding contact angle, 'Δρ' is the CO_2-brine density difference, 'g' is the gravitational acceleration, and 'R' is the caprock's average pore throat radius.

Thus, for a limestone storage formation at 10 MPa and 323 K, three main cases can be distinguished: a) pure calcite, b) storage rock exposed to 10^{-6} M stearic acid, and c) storage rock exposed to 10^{-2} M stearic acid.

The corresponding 'θ_r' values under these conditions are 45°, 55° and 100° (Figure 1). The 'γ' and 'Δρ' values at 10 MPa and 323 K are 40 mN/m from[69] and 683 kg/m^3 interpolated from[70] respectively; while a typical caprock pore radius is 0.01 µm from[71]. CO_2 column heights 'h' calculated using Eq. (1) are thus 916 m for the case of pure calcite, 685 m for the case of 10^{-6} M stearic acid exposure, and -207 m for the calcite surface exposed to 10^{-2} M stearic acid (Figure 4). It is therefore clear that with increasing stearic acid concentration, the structural storage capacity reduces significantly. Moreover, the column height reached a negative value (-207 m) at 10^{-2} M stearic acid concentration, indicating CO_2 leakage due to wettability reversal (Figure 4).

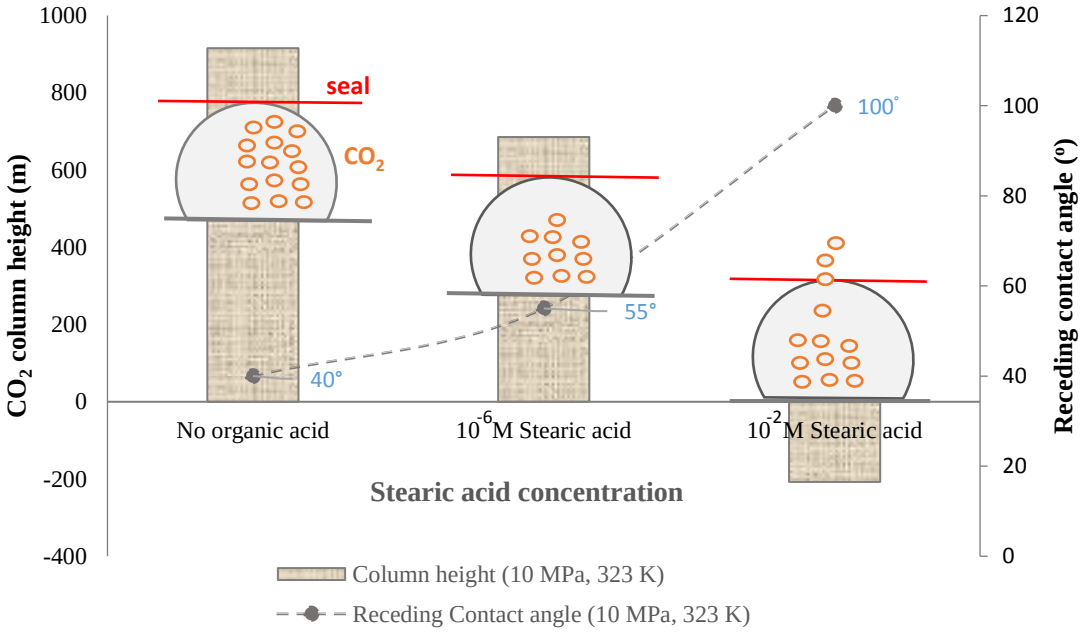

Figure 4. CO_2 column heights estimated as a function of stearic acid concentration at 10 MPa and 323 K. For 10^{-2} M stearic acid concentration, the height is negative which implies CO_2 leakage (column in negative y-axis). The graphic at the intersect of each column illustrates a hypothetical storage scenario where the black semi-circular region represents the storage rock, orange bubbles inside represent CO_2, and the red line at the top represents the seal layer. The left column (no organic present) shows CO_2 bubbles occupying a larger height as compared to the second column, which indicates a decrease in structural trapping due to presence of organic acid, whereas the column on the right shows potential CO_2 leakage due to wetting alteration to weakly CO_2-wet at higher organic acid concentrations.

Furthermore, the wettability alteration found in this work can be explained by the interplay of the interfacial tensions ('γ') which are related by the Young's equation as follows[72]:

$$\cos\theta = \frac{\gamma_{sv} - \gamma_{sl}}{\gamma_{vl}} \qquad Eq.2)$$

In Eq. (2), 'γ_{sv}' is the calcite-CO_2 interfacial tension, 'γ_{sl}' is the calcite-brine interfacial tension, and 'γ_{vl}' is the CO_2-brine interfacial tension. At a given pressure and temperature, the numerator in equation (2) decreases with increasing stearic acid concentration as 'γ_{sv}' decreases with increasing stearic acid coverage[14,69]. Thus, as 'γ_{vl}' is a constant at constant pressure and temperature, the adsorption of stearic acid on the calcite surface results in a higher water contact angle and de-wetting of the surface.

It is thus clear that a precise knowledge of the organic acid concentrations in a storage reservoir is essential for assessing the conditions for long-term geological storage. A pertinent limitation, however, is that current data applies to carbonate/limestone formations, and a broader consideration of various organic acid molecules and minerals may provide better insights. Moreover, We note that it has been previously shown for quartz surfaces that divalent cations result in further contact angle increase due to the stronger surface screening effect of the divalent ions (in comparison with the corresponding monovalent ions), thus reducing the surface potential and surface hydrophilicity – which results in higher contact angles[4,17].

4. Conclusions

Deep saline aquifers and depleted hydrocarbon reservoirs are the most important sinks for CO_2 geological storage.[1,73] However, it has been shown that the CO_2-wettability of the storage and seal rock dramatically influences the injectivity, storage capacity, containment security,[4,5,9,34,35,64,65] and thus project economics and technical feasibility.

Realistic subsurface conditions have, however, not been tested, and the focus was on clean mineral substrates, which, however, do not exist in the subsurface (as in the subsurface anoxic or reducing conditions prevail, while clean mineral surfaces can only exist in strongly oxidising conditions).[18,20]

We therefore measured the CO_2-wettability on carbonate mineral surfaces which mimic these subsurface storage conditions of carbonate reservoirs more realistically. This representativeness was achieved by exposure to a highly diluted carboxylic acids (10^{-2} – 10^{-10} M), and measurements were conducted at realistic storage conditions (10 MPa and 25 MPa and 323 K). Clearly, even minute exposure to traces of such organic acid molecules significantly increased the water contact angle (θ), and thus CO_2-wettability. This effect drastically increased with higher organic acid concentration and pressure.

We thus conclude that CO_2 geological storage capacities and containment security can be significantly lower than previously thought. Reservoir-scale models thus need to take these effects into account so that accurate storage predictions are obtained thus de-risking carbon geological storage (CGS) projects.

Conflicts of Interest

There are no conflicts to declare.

Acknowledgments

The first author acknowledges the support provided from the Australian Government and Curtin University for providing Research Training Program Scholarship for his research studies. The authors declare no competing financial interests.

References

1. Intergovernmental Panel on Climate Change (IPCC) (2005), IPCC Special Report on Carbon Dioxide Capture and Storage. Prepared by Working Group III of the Intergovernmental Panel on Climate Change, edited by B. Metz et al., Cambridge Univ. Press, Cambridge, United Kingdom, and New York, USA.

2. F. M. Orr, Onshore geologic storage of CO_2, Science, 2009, 325(5948), 1656-1658.

3. C. R. Jenkins, P. J. Cook, J. Ennis-King, J. Undershultz, C. Boreham, T. Dance, T., ... and D. Kirste, Safe storage and effective monitoring of CO_2 in depleted gas fields. Proc. Natl. Acad. Sci. U. S. A., 2012, 109(2), E35-E41.

4. S. Iglauer, CO_2–Water–Rock Wettability: Variability, Influencing Factors, and Implications for CO_2 Geostorage, Acc. Chem. Res., 2017, 50(5), 1134-1142.

5. S. Iglauer, C. H. Pentland and A. Busch, CO_2 wettability of seal and reservoir rocks and the implications for carbon geo-sequestration, Water Resour. Res., 2015, 51(1), 729-774.

6. K. Chaudhary, M. Bayani Cardenas, W. W. Wolfe,J.A. Maisano, R.A. Ketcham and P.C. Bennett, Pore-scale trapping of supercritical CO_2 and the role of grain wettability and shape. Geophys. Res. Lett., 2013, 40(15), 3878-3882.

7. A. S. Al-Menhali, H. P. Menke, M. J. Blunt and S. C. Krevor, Pore Scale Observations of Trapped CO_2 in Mixed-Wet Carbonate Rock: Applications to Storage in Oil Fields, Enviro$_n$. Sci. Technol., 2016, 50(18), 10282-10290.

8. T. Rahman, M. Lebedev, A. Barifcani and S. Iglauer, Residual trapping of supercritical CO_2 in oil-wet sandstone, J. Colloid Interface Sci., 2016, 469, 63-68.

9. E. A. Al-Khdheeawi, S. Vialle, A. Barifcani, M. Sarmadivaleh and S. Iglauer, Impact of reservoir wettability and heterogeneity on CO_2-plume migration and trapping capacity, Int. J. Greenhouse Gas Control, 2017, 58, 142-158.

10. R. Farokhpoor, B. J. Bjørkvik, E. Lindeberg and O. Torsæter, Wettability behaviour of CO_2 at storage conditions, Int. J. Greenhouse Gas Control, 2013, 12, 18-25.

11. S. Saraji, M. Piri and L. Goual, The effects of SO2 contamination, brine salinity, pressure, and temperature on dynamic contact angles and interfacial tension of supercritical CO_2/brine/quartz systems, Int. J. Greenhouse Gas Control, 2014, 28, 147-155.

12. D. N. Espinoza and J. C. Santamarina, Water-CO_2-mineral systems: Interfacial tension, contact angle, and diffusion—Implications to CO_2 geological storage, Water Resour. Res., 2010, 46(7).

13. D. Broseta, N. Tonnet and V. Shah, Are rocks still water-wet in the presence of dense CO_2 or H_2S?, Geofluids, 2012, 12(4), 280-294.

14. J. L. Dickson, G. Gupta, T. S. Horozov, B. Binks and K. P. Johnston, Wetting phenomena at the CO_2/water/glass interface, Langmuir, 2006, 22(5), 2161-2170.

15. D. Yang, Y. Gu and P. Tontiwachwuthikul, Wettability determination of the reservoir brine− reservoir rock system with dissolution of CO_2 at high pressures and elevated temperatures, Energy Fuels, 2007, 22(1), 504-509.

16. C. Chen, J. Wan, W. Li and Y. Song, Water contact angles on quartz surfaces under supercritical CO_2 sequestration conditions: Experimental and molecular dynamics simulation studies, Int. J. Greenhouse Gas Control, 2015, 42, 655-665.

17. A. Z. Al-Yaseri, M. Lebedev, A. Barifcani and S. Iglauer, Receding and advancing (CO_2+ brine+ quartz) contact angles as a function of pressure, temperature, surface roughness, salt type and salinity, J. Chem. Thermodyn., 2016, 93, 416-423.

18. J. C. Love, L. A. Estroff, J. K. Kriebel, R. G. Nuzzo and G. M. Whitesides, Self-assembled monolayers of thiolates on metals as a form of nanotechnology, Chem. Rev., 2005, 105(4), 1103-1170.

19. S. Iglauer, A. Salamah, M. Sarmadivaleh, K. Liu and C. Phan, Contamination of silica surfaces: impact on water–CO_2–quartz and glass contact angle measurements, Int. J. Greenhouse Gas Control, 2014, 22, 325-328.

20. P. Froelich, G. P. Klinkhammer, M. L. Bender, N. A. Luedtke, G. R. Heath, D. Cullen ... and V. Maynard, Early oxidation of organic matter in pelagic sediments of the eastern equatorial Atlantic: suboxic diagenesis, Geochim. Cosmochim. Acta, 1979, 43(7), 1075-1090.

21. G. T. Townsend, R. C. Prince and J. M. Suflita, Anaerobic oxidation of crude oil hydrocarbons by the resident microorganisms of a contaminated anoxic aquifer. Environ, Sci. Technol., 2003, 37(22), 5213-5218.

22. Y. K. Kharaka, J. J. Thordsen, S. D. Hovorka, H. S. Nance, D. R. Cole, T. J. Phelps and K. G. Knauss, Potential environmental issues of CO_2 storage in deep saline aquifers: geochemical results from the Frio-I Brine Pilot test, Texas, USA, Appl. Geochem., 2009, 24(6), 1106-1112.

23. L. Stalker, S. Varma, D. Van Gent, J. Haworth and S. Sharma, South West Hub: a carbon capture and storage project, Aust. J. Earth Sci., 2013, 60(1), 45-58.

24. P. M. Jardine, J. F. McCarthy and N. L. Weber, Mechanisms of dissolved organic carbon adsorption on soil, Soil Sci. Soc. Am. J., 1989, 53(5), 1378-1385.

25. L. Madsen and L. Ida, Adsorption of carboxylic acids on reservoir minerals from organic and aqueous phase, SPE Reservoir Eval. Eng., 1998, 1(01), 47-51.

26. L. Yang, T. Xu, M. Wei, G. Feng, F. Wang and K. Wang, Dissolution of arkose in dilute acetic acid solution under conditions relevant to burial diagenesis, Appl. Geochem., 2015, 54, 65-73.

27. E. M. Thurman, Organic geochemistry of natural waters, Springer Netherlands, 1985, (pp. 151-180).

28. W. Adamson and A. P. Gast, Phys. Chem. Surf., 6th ed., Wiley-Interscience, N. Y, 1997.

29. G. L. Gaines, Insoluble monolayers at liquid-gas interfaces, Interscience Publishers, New York, 1966.

30. J. A. Zasadzinski, R. Viswanathan, L. Madsen, J. Garnaes and D. K. Schwartz, Langmuir-Blodgett films, Science (Washington, D.C.), 1994, 263, 1726 – 1733.

31. E. G. Shafrin and W. A. Zisman, Effect of progressive fluorination of a fatty acid on the wettability of its adsorbed monolayer, The J. Physical Chem., 1962, 66(4), 740-748.

32. H. Kuhn and D. Möbius, Systems of monomolecular layers—Assembling and physico-chemical behavior, Angew. Chem., Int. Ed. Engl., 1971, 10(9), 620-637.

33. R. Maboudian and R.T. Howe, Critical review: adhesion in surface micromechanical structures, J. Vac. Sci. Technol., 1997, B 15, 1 – 20.

34. E. A. Al-Khdheeawi, S. Vialle, A. Barifcani, M. Sarmadivaleh and S. Iglauer, Influence of CO_2-wettability on CO_2 migration and trapping capacity in deep saline aquifers, Greenhouse Gases: Sci. Technol., 2017, 7(2), 328-338.

35. S. Iglauer, A. Z. Al-Yaseri, R. Rezaee and M. Lebedev, CO_2 wettability of caprocks: Implications for structural storage capacity and containment security, Geophys. Res. Lett., 2015, 42(21), 9279-9284.

36. A. Venkatraman, L. W. Lake and R. T. Johns, Gibbs free energy minimization for prediction of solubility of acid gases in water, Ind. Eng. Chem. Res., 2014, 53(14), 6157-6168.

37. A. Alroudhan, J. Vinogradov and M. D. Jackson, Zeta potential of intact natural limestone: Impact of potential-determining ions Ca, Mg and SO_4, Colloids Surf., A, 2016, 493, 83-98.

38. R. M. El-Maghraby, C. H. Pentland, S. Iglauer and M. J. Blunt, A fast method to equilibrate carbon dioxide with brine at high pressure and elevated temperature including solubility measurements, The Journal of Supercritical Fluids, 2012, 62, 55-59.

39. V. A. Tabrizy, R. Denoyel and A. A. Hamouda, Characterization of wettability alteration of calcite, quartz and kaolinite: Surface energy analysis, Colloids Surf., A, 2011, 384(1), 98-108.

40. O. Karoussi, L. L. Skovbjerg, T. Hassenkam, S. S. Stipp and A. A. Hamouda, AFM study of calcite surface exposed to stearic and heptanoic acids, Colloids Surf., A, 2008, 325(3), 107-114.

41. H. J. Ulrich, W. Stumm and B. Cosovic, Adsorption of aliphatic fatty acids on aquatic interfaces. Comparison between two model surfaces: the mercury electrode and δ-Al2O3 colloids, Environ. Sci. Technol., 1988, 22(1), 37-41.

42. J. J. Zullig and J. W. Morse, Interaction of organic acids with carbonate mineral surfaces in seawater and related solutions: I. Fatty acid adsorption, Geochim. Cosmochim. Acta, 1988, 52(6), 1667-1678.

43. M. Ochs, B. Ćosović and W. Stumm, Coordinative and hydrophobic interaction of humic substances with hydrophilic Al2O3 and hydrophobic mercury surfaces, Geochim. Cosmochim. Acta, 1994, 58(2), 639-650.

44. M. Kleber, K. Eusterhues, M. Keiluweit, C. Mikutta, R. Mikutta and P. S. Nico, Mineral–organic associations: formation, properties and relevance in soil environments, Adv. Agron., 2015, 130, 1-140.

45. J. A. Davis, Adsorption of natural dissolved organic matter at the oxide/water interface, Geochim. Cosmochim. Acta, 1982, 46(11), 2381-2393.

46. X. Ji and C. Zhu, CO_2 storage in deep saline aquifers. Chapter 10 in Novel Mater, Carbon Dioxide Mitigation Technol., 2015, 299-332.

47. J. T. Birkholzer, Q. Zhou and C. F. Tsang, Large-scale impact of CO_2 storage in deep saline aquifers: a sensitivity study on pressure response in stratified systems, Int. J. Greenhouse Gas Control, 2009, 3(2), 181-194.

48. J. M. Nordbotten, M. A. Celia and S. Bachu, Injection and storage of CO_2 in deep saline aquifers: analytical solution for CO_2 plume evolution during injection, Transp. Porous Media, 2005, 58(3), 339-360.

49. C. M. White, B. R. Strazisar, E. J. Granite, J. S. Hoffman and H. W. Pennline, Separation and capture of CO_2 from large stationary sources and sequestration in geological formations—coalbeds and deep saline aquifers, J. Air Waste Manage. Assoc., 2003, 53(6), 645-715.

50. S. Hoeiland, T. Barth, A. M. Blokhus and A. Skauge, The effect of crude oil acid fractions on wettability as studied by interfacial tension and contact angles, J. Pet. Sci. Eng., 2001, 30(2), 91-103.

51. K. R. Gomari and A. A. Hamouda, Effect of fatty acids, water composition and pH on the wettability alteration of calcite surface, J. Pet. Sci. Eng., 2006, 50(2), 140-150.

52. A. A. Hamouda and K. A. Rezaei Gomari, Influence of temperature on wettability alteration of carbonate reservoirs, SPE/DOE Symposium on Improved Oil Recovery, Soc. Pet. Eng., 2006, doi: 10.2118/99848-MS.

53. P. C. Bennett, D. E. Siegel, M. J. Baedecker and M. F. Hult, Crude oil in a shallow sand and gravel aquifer—I. Hydrogeology and inorganic geochemistry. Appl. Geochem., 1993, 8(6), 529-549.

54. D. M. Jones, I. M. Head, N. D. Gray, J. J. Adams, A. K. Rowan, C. M. Aitken ... and T. Oldenburg, Crude-oil biodegradation via methanogenesis in subsurface petroleum reservoirs. Nat., 2008, 451(7175), 176.

55. S. R. Mihajlović, D. R, Vučinić, Ž. T. Sekulić, S. Z. Milićević and B. M. Kolonja, Mechanism of stearic acid adsorption to calcite, Powder Technol., 2013, 245, 208-216.

56. F. Heberling, T. P. Trainor, J. Lützenkirchen, P. Eng, M. A. Denecke and D. Bosbach, Structure and reactivity of the calcite–water interface, J. Colloid Interface Sci., 2011, 354(2), 843-857.

57. X. Shi, R. Rosa and A. Lazzeri, On the coating of precipitated calcium carbonate with stearic acid in aqueous medium, Langmuir, 2010, 26(11), 8474-8482.

58. C. Wang, Y. Sheng, X. Zhao, Y. Pan and Z. Wang, Synthesis of hydrophobic CaCO3 nanoparticles, Mater. Lett., 2006, 60(6), 854-857.

59. Z. Cao, M. Daly, L. Clémence, L. M. Geever, I. Major, C. L. Higginbotham and D. M. Devine, Chemical surface modification of calcium carbonate particles with stearic acid using different treating methods, Appl. Surf. Sci., 2016, 378, 320-329.

60. S. Al-Anssari, A. Barifcani, S. Wang and S. Iglauer, Wettability alteration of oil-wet carbonate by silica nanofluid, J. Colloid Interface Sci., 2016, 461, 435-442.

61. M. Arif, M. Lebedev, A. Barifcani and S. Iglauer, CO_2 storage in carbonates: Wettability of calcite, Int. J. Greenhouse Gas Control, 2017, 62, 113-121.

62. S. Al-Anssari, M. Arif, S. Wang, A. Barifcani, M. Lebedev and S. Iglauer, CO_2 geo-storage capacity enhancement via nanofluid priming, Int. J. Greenhouse Gas Control., 2017, 63, 20-25.

63. L. M. Lander, L. M. Siewierski, W. J. Brittain and E. A. Vogler, A systematic comparison of contact angle methods, Langmuir, 1993, 9(8), 2237-2239.

64. M. Arif, A. Barifcani, M. Lebedev and S. Iglauer, Structural trapping capacity of oil-wet caprock as a function of pressure, temperature and salinity, Int. J. Greenhouse Gas Control, 2016, 50, 112-120.

65. M. Arif, M. Lebedev, A. Barifcani and S. Iglauer, Influence of shale-total organic content on CO_2 geo-storage potential, Geophys. Res. Lett., 2017, 44, GL073532.

66. P. Chiquet, D. Broseta and S. Thibeau, Wettability alteration of caprock minerals by carbon dioxide, Geofluids, 2007, 7(2), 112-122.

67. M. Naylor, M. Wilkinson and R. S. Haszeldine, Calculation of CO_2 column heights in depleted gas fields from known pre-production gas column heights, Mar. Pet. Geol., 2011, 28(5), 1083-1093.

68. N. R. Morrow, Physics and thermodynamics of capillary action in porous media, Ind. Eng. Chem., 62(6), 32-56.

69. M. Arif, F. Jones, A. Barifcani, and S. Iglauer, Electrochemical investigation of the effect of temperature, salinity and salt type on brine/mineral interfacial properties, Int. J. Greenhouse Gas Control, 2017, 59, 136-147.

70. X. Li, E. Boek, G. C. Maitland, & J. M. Trusler, Interfacial Tension of (Brines+ CO_2):(0.864 NaCl+ 0.136 KCl) at Temperatures between (298 and 448) K, Pressures between (2 and 50) MPa, and Total Molalities of (1 to 5) mol· kg–1. J. Chem. Eng. Data, 2012, 57(4), 1078-1088.

71. P. H. Nelson, Pore-throat sizes in sandstones, tight sandstones, and shales, AAPG bulletin, 2009, 93(3), 329-340.

72. M. Arif, A. Barifcani, and S. Iglauer, Solid/CO_2 and solid/water interfacial tensions as a function of pressure, temperature, salinity and mineral type: Implications for CO_2-wettability and CO_2 geo-storage, Int. J. Greenhouse Gas Control, 2016, 53, 263-273.

73. A. Firoozabadi and P. C. Myint, Prospects for subsurface CO_2 sequestration, AIChE j., 2010, 56(6), 1398-1405.